Cool Skins:
Materials and Assemblies for Ventilated Building Envelopes in Warm Climates

Michael D. Gibson[1]

ABSTRACT:
Vertical building skins account for a significant amount of heat transfer from solar gain in the cooling season, especially in multi-floor, envelope load dominated buildings in sunny climates. While the performance of glazing with respect to solar radiation is often given the greatest emphasis, the behavior of the opaque building envelope is also an important factor in cooling season performance. Conventionally, buildings approach this problem in the envelope using just insulation.

Ventilated cladding systems can improve the performance of light-weight assemblies in the cooling season, though ventilated cladding is a strategy more widely associated with moisture evacuation. Using mockups and CFD simulation, the author has observed heat transfer rates reduced by over 40% by ventilating the building cladding to the exterior. Earlier published findings from the author suggest that the dynamic thermal behavior of these ventilated skins is complex and may be best optimized by using heat-rejecting materials and open joints, countering prevailing research on the subject asserting that only the parameters of the air channel are the critical values for optimization.

This paper presents a new phase of inquiry that further characterizes the thermal behavior of ventilated building skins, with special emphasis on the role of radiation, cladding equilibrium temperature, and behavior of the cladding as an assembly with continuous external insulation. New findings reinforce the importance of light weight cladding in rejecting solar heat gain, discuss the impact of insulation on cladding thermal behavior, and argue for the use of metal cladding as the best-performing 'cool skin'. Lastly the current work explores annual cooling performance impacts of ventilated cladding using whole building energy modeling that considers radiation and cladding equilibrium temperature as the dominant performance factors for cool skins.

1.0 INTRODUCTION

For decades, ventilated cladding systems have been used in buildings as a strategy for moisture remediation. In these systems, also referred to as rainscreen cladding systems, the cladding of the building is separated from the drainage plane (i.e. weather barrier) in the wall assembly and a system of openings vent the cladding to the outside environment. In principle, ventilating the cladding allows liquid moisture and vapor out of the wall assembly before it can migrate into the interior wall cavity. The concept of using ventilated cladding to slow down the transmission of heat gain in the cooling season is similar to the way in which rainscreen walls reject moisture. Radiation that would otherwise be conducting to the interior of the building is rejected, in part, by the ventilated cladding and released to the exterior of the building (see "Cool Skin" in Figure 1). The prevailing school of thought on ventilated cladding for cooling emphasizes the air cavity behind the cladding as the area of primary interest (see Ciampi 2003, Suarez 2011, Marinosci 2011, and Giancolaa 2012), dedicating less discussion to the cladding itself. This paper intends to characterize the subject of ventilated cladding for cooling in a different manner, emphasizing the role of cladding equilibrium temperature in reducing heat transfer through the wall assembly.

[1]Michael D. Gibson, Assoc. AIA, LEED A.P.; Assistant Professor, Dept. of Architecture, Kansas State University

1.1 Hot Skins versus Cool Skins

The cooling season performance differences between non-ventilated and ventilated cladding can be described first using a simple expressions of heat flow. When the building cladding is subjected to solar radiation (insolation), radiation is absorbed and the cladding heats up as the incoming heat flow outpaces the heat loss from the cladding as a result of convection and radiation back to the exterior environment. Conduction of heat to the interior of the building, which we may presume because of climate control is cooler than the exterior temperature, would also be heat 'loss' with respect to the cladding. The equation below (eq. 1) describes this mechanism of heat gain and loss, with $\dot{q}_{net}$ resulting.

$$\dot{q}_{net} = \dot{q}_{gain} - \dot{q}_{loss} \qquad \text{(EQ. 1)}$$

When $\dot{q}_{net}$ is positive, excess heat flow will raise the cladding system's temperature until losses once again equal gains, and the temperature of the cladding stabilizes at equilibrium temperature ($\dot{q}_{net} = 0$). In the equation above, heat losses include heat transfer both back to the environment and into the cooler building. This condition illustrates the problem of conceptualizing heat gain acting on the building skins, which is very different than the steady state heat loss in the heating season. In the heating season, insulation is an important useful mitigating strategy, since adding insulation to the wall assembly slows down the flow of heat to the exterior. In the cooling season when gain is coming from the outside, insulation slowing down heat transfer to the interior (a component of $\dot{q}_{loss}$ from eq. 1) tends to increase equilibrium temperature by increasing $\dot{q}_{net}$ in the cladding for the same incoming insolation. Resultant heat in the cladding is nonetheless conducted through the wall assembly where it impacts the interior as heat gain by conduction, with the magnitude of heat transfer influenced directly by the subsequent temperature difference between interior and exterior (Eq. 2).

$$q = kA\frac{(T_1 - T_2)}{L} \qquad \text{(EQ. 2)}$$

Thus insulation intended to slow heat loss in the winter time contributes to higher cladding temperatures in the cooling season. While traditional buildings used massive construction (uninsulated stone and masonry) to temper heat gain in the envelope, modern light weight buildings distinguish cladding from structure, thermally isolating it with insulation. In climates with significant solar heat gain, the isolated cladding can reach very high temperatures, observed in the field during earlier research, climbing to over 180°F (82°C) on vertical walls. This condition is illustrated in Fig. 1 as the 'hot skin' condition. Conventional building science and computer modeling represents this condition as Sol-Air heat transfer (Eq. 3), where the magnitude of incident solar radiation and cladding thermal resistance is used to calculate an equivalent exterior temperature, aggregating heat flow from the exterior air with the impact of solar radiation. The resultant temperature is then used to calculate heat flow via the conventional conduction calculation (Eq. 2).

$$T_{Sol\text{-}Air} = T_{AO} + R_{SO} \quad (\alpha \cdot G)^* \qquad \text{(EQ. 3)}$$

Whereby
- $T_{Sol\text{-}Air}$ = the sol-air temperature, used to calculate heat transfer by conduction
- T_{AO} = temperature of air outside
- R_{SO} = resistance of outside (cladding) surface, ℓ /k
- α = absorptivity of outside (cladding) surface
- G = incident solar radiation

* This version of the sol-air equation does not account for radiation exchange with exterior bodies, though in some applications this is introduced along with absorbed incident solar radiation.

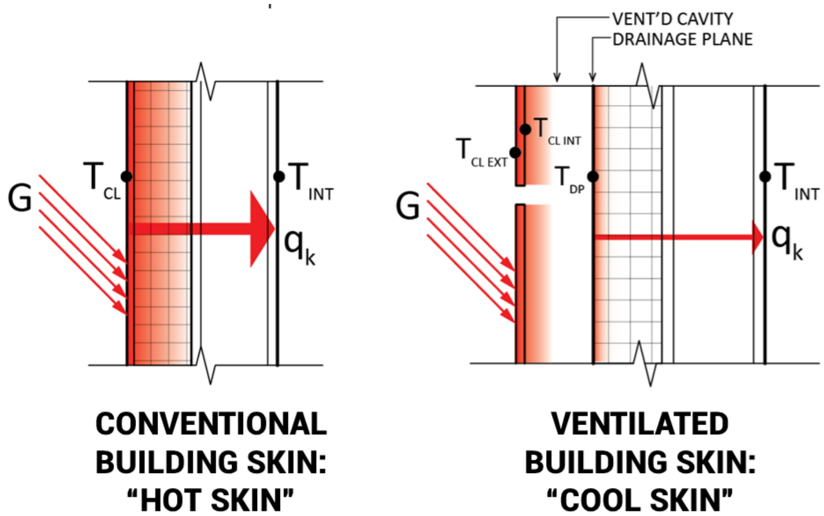

Figure 1: Heat flow characteristics in a typical, non-ventilated wall (L) and a ventilated cladding wall (R). In the ventilated example, $T_{CL\ EXT}$ and $T_{CL\ INT}$ are the temperatures at the exterior and interior of the cladding respectively, and T_{DP} is the temperature at the drainage plane, at which conductive heat transfer through the building envelope begins.

The Sol-Air model is only a rough predictor of cladding temperature because it does not factor in additional heat losses to the exterior by convection and radiation; however the use of the Sol-Air model in computer simulation allows a close approximation of how solar radiation is transmitted through the opaque parts of building envelopes. Consider the example of a generic four-level office building with a footprint of 80 feet by 60 feet, and located in Houston, Texas (Fig. 2). Sol-Air heat gains (insolation transmitted through opaque envelope surfaces) comprise 15.5% of overall annual gains, without considering internal loads. Separating the roof from this number, the vertical walls contribute to 7.1% of overall annual gains. As a multi-floor building, we can further isolate its second floor as a thermal zone and see that over the course of the year, Sol-Air gains make up a maximum of 23% of gains in the Spring and Fall transition seasons and a minimum of 3% of gains when exterior air temperature (conduction, ventilation gain) and relative humidity (ventilation gain) have a dominant impact on cooling load. Sol-Air gains in this zone also composed 21% of the maximum cooling rate in the simulation, which is higher (by 24%) than direct solar gains through glass. Thus for warm and sunny climates, if insolation can be better mitigated in vertical building envelopes, a significant amount of cooling energy use can be reduced especially during the transition seasons and during peak cooling, and particularly for thermal zones that are decoupled from roofs (i.e. lower floors in multifloor buildings).

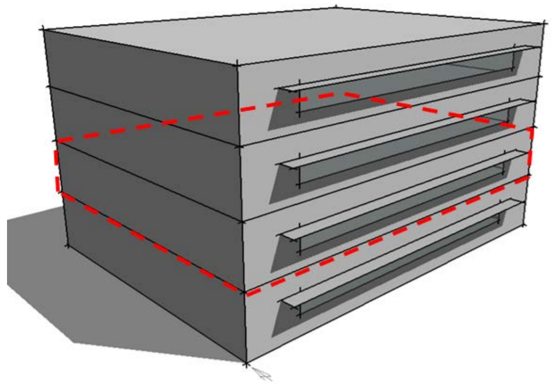

Figure 2: A generic commercial building located in Houston, TX. A mid-level thermal zone receives approx. 21% of its peak cooling from solar radiation impacting its opaque envelope. Better performing "cool skins" can mitigate this cooling load.

Recalling Eq. 1, we may reduce $\dot{q}_{gain}$ in the cladding by making it less absorptive with respect to insolation, thus reaching the condition of equilibrium ($\dot{q}_{net}$ = 0) at a lower temperature. Ventilating the cladding by separating it from the backup wall offers a different opportunity on the side of $\dot{q}_{loss}$. As discussed earlier, heat gained by unventilated cladding can only be released to the exterior side by convection and radiation and through the interior wall by conduction. When the cladding is ventilated, it can release heat from both sides via convection and radiation (Fig 1), greatly increasing the magnitude of $\dot{q}_{loss}$ and leading to the condition of equilibrium ($\dot{q}_{net}$ = 0) at a lower temperature. Though reducing the absorptivity of the cladding (i.e. using lighter cladding colors) by itself is an easy first step, including the additional measure of cladding ventilation results in the greatest reduction in cladding temperature.

The area of greatest concern with respect to heat transfer through ventilated cladding assemblies is the temperature of the drainage plane (i.e. back up wall surface) because it is this temperature that ultimately influences the amount of heat transferred by conduction to the interior (via Eq. 2). Heat from the cladding is transferred either to the exterior of the building or to the cavity; heat transferred to the cavity air column subsequently either exits the cavity or is transferred to the drainage plain by a combination of conduction, convection and radiation (Fig. 1). In lieu of describing the mechanisms of heat transfer with precision, the opportunity to release heat from the cladding on each side lowers its temperature and rejects some amount of heat gain. While this amount of heat is practically limited in magnitude to the insolation heat gain (i.e. it cannot cool the exterior wall below ambient temperature), as a cost-neutral enhancement to the cladding this approach presents a logical way of reducing cooling season loads.

2.0 BACKGROUND

2.1 Prior Research on Ventilated Cladding

The benefits of ventilating building enclosures were initially identified with ventilated roofing, with research in this area indicating clear energy saving potential for releasing heat gain from behind the roofing using vented cavities (Ciampi 2005). After many years, this installation method for metal roofs has become more popular. Thermal buoyancy, the driving mechanism of heat-induced ventilation, causes air to flow upwards in the cavity towards the higher vent; yet this heated air also tends, due to gravity, to flow with more proximity to the heated roof surface and away from the roofing substrate on the interior side of the cavity.

Ventilated cladding systems, while working under the same premise as ventilated roofs, have some important differences. In roofs, heat gain and resultant temperatures are much higher than in walls because of the intensity of solar radiation and the higher radiation incidence angle that corresponds more to roof orientations than walls. Additionally, roofs are intended to be water impenetrable and thus are tightly constructed between the upper and lower terminations where they may be vented; as a result of this tightness, ventilation is based on the thermosiphon effect, where differences in temperature at an upper outlet drive flow throughout the system. In contrast to roofs, walls can become very hot but do not receive the same magnitude of insolation as roofs do. Ventilated walls are also not typically constructed as continuous barriers and usually have some degree of open and/or unsealed joints interspersed throughout their height.

Recent research from scientists in the Mediterranean region focused on cementitious, ceramic, and cultured stone ventilated claddings (see Ciampi 2003, Suarez 2011, Marinosci 2011, and Giancolaa 2012) and shared the common approach of studying heat transfer mechanisms in the air cavity behind the cladding. Marinosci (2011) and Giancolaa (2012) compared empirical experiments comparing observations of large-scale ventilated cladding walls with the results computer simulations. Ciampi (2003) developed a heat transfer model based on convective heat transfer by mass flow and applied the model to cooling optimization problems involving cavity depth and cladding material. Suarez (2011) correlated results of mass flow calculations with computer simulations in order to further develop convection coefficients that can be applied to asymmetrically heated cladding conditions.

In lieu of dissecting the content and conclusions of the above papers, it is important to note the great effort of this previous research towards predicting the heat transfer and general behavior of the air channel in the cavity. The assertion made is that heat transfer in ventilated cladding systems can be accurately modeled using equations applicable to a fluid moving through parallel plates, a model that generalizing the behavior of the air mass in the cavity as mass flow. For several reasons this mass flow model presents an incomplete picture of the behavior of ventilated skins. Suarez (2011) argued that the prevailing ventilated cladding models based on mass flow were based on symmetrical heating in the air cavity, differing from the actual conditions in air cavities which would typically be asymmetrically heated, with much greater heat entering the system on the cladding side. Suarez (2011) also argued that generalizing the air flow in an entire vertical wall based on limited conditions at inlets, outlets, and arbitrary intermediate points. Of the previous articles cited, three of these studies (Ciampi 2003, Suarez 2011, Marinosci 2011) omitted the potential impact of open, unsealed joints in the mathematical models and computer simulations.

In 2012, this author conducted a series of experiments in order to test the hypothesis that ventilated cladding systems with open joints would perform less heat rejection than ventilated cladding systems whose joints, with the exception of the bottom inlet and top outlet, were closed. A third system of non-ventilated cladding was tested with the open and closed joint variations, and these systems were tested in an environmentally controlled test chamber, in outdoor tests, and using computer-based computational fluid dynamics (CFD) simulation. While both open and closed joint ventilated cladding systems performed better than non-ventilated cladding in rejecting solar heat gain during all tests, the open joint system unexpectedly outperformed the closed joint system by producing lower drainage plane temperatures and lower cladding temperatures. The unexpected success of the open joint system revealed that the behavior of the ventilated cladding system was more complex than the mass flow models presented in the literature. (Gibson 2013)

Closer examination of the open joint and closed joint system with finer-grain CFD simulation revealed that in the closed joint system, air flow in the cavity was actually relatively slow and with respect to the cross section of the cavity, air was practically still at the cladding and drainage plane surfaces – a pattern also verified in a second round of live testing using instrumentation. This pattern is a classic example of low-speed laminar flow, where a stable air flow is flanked by films of air that decrease in velocity towards the boundary surfaces. Under realistic conditions, the air in the cavity of the closed joint system was not only warmer than the open joint model, but also moved much more slowly overall. The air column itself also began at the base of the wall with no detectable velocity at the bottom and accelerated with height to a maximum velocity at the outlet. In contrast, the open joint cladding system exhibited flow in the cavity that was at a higher velocity and was more turbulent, forcing the moving air column into contact with the cladding and the drainage plane. Moreover, air entered and exited the cavity through the intermediate joints as well as the inlet and outlet, moving more air through the cavity while also resulting in some additional edge cooling of the cladding panels. Wind, in real life applications, would provide the open joint system would additional ventilation to improve its performance over closed joint systems. In summary, the open-joint system moved more heat from the cladding and cavity and consequently transferred less heat to the drainage plane than the system using closed joints.

Figure 3: Outdoor test, conducted over the course of four hours in September with mostly sunny conditions and an ambient temperature ranging from 94F to 102.7F. Comparing average temperatures at hour 4 measured at the drainage plane, the unventilated cladding wall measured 119.5F, the closed joint ventilated cladding wall measured 109.4F, and the open joint ventilated cladding wall measured 107.1F.

2.2 Equilibrium Temperature versus Mass Flow Model

The research question of open versus closed joints originally proposed by this author was inspired by an increasing trend in rainscreen cladding in the United States which uses ventilated light-weight metals, fibrous, and cementitious panels that are offset from the drainage plane of the wall assembly, often with a significant amount of exterior insulation preceding the sheathing and wall structure. This type of building system is substantially different from the heavier cladding systems studied in the earlier mentioned Mediterranean research (Marinosci 2011, and Giancolaa 2012). Ciampi's (2003) optimization, using his mass-flow model, concluded that a brick exterior wall of 5cm thickness would result in the best cooling performance, exceeding a variety of metal and composite materials. It is presumed this conclusion was reached based on the role in the thermal model attributed to the thermal resistance (influencing conduction through and radiation to and from) and heat transfer coefficients (influencing convection) of the cladding material, which favors a more thermally resistant cladding with a higher heat transfer coefficient (Ciampi 2003). This is a product, however, of a numerical model that focuses on the air cavity as the critical area of performance in the ventilated cladding system.

On the other hand, this author's conclusion that open joints rejected more heat from the wall system raised a question about whether the idealized convection of the mass flow model was useful in improving a light-weight ventilated cladding system designed around frequent open joints. In response, a new research question was formulated around the cladding material. How would material variations – particularly with respect to weight – influence the performance of ventilated cladding?

The specific mathematical model from Ciampi (2003) assumed steady state temperature conditions based on sol-air temperature of the cladding but did not consider the dynamic thermal effects by which insolation impacts cladding temperature. Sol-air temperature is useful for predicting the exposed surface temperature of material that conducts its heat through a larger assembly. Yet heat gain that is not balanced by heat, recalling Eq. 1, results in $\dot{q}_{net}$, leading to a subsequent rise in cladding temperature as a result of stored energy. This process of gaining and shedding heat ends in thermal equilibrium (where $\dot{q}_{net} = 0$) that sets the temperature of the cladding within the wall cavity. The question may then be posed: what is the role of cladding equilibrium temperature with respect to cooling performance, and is potential role of equilibrium temperature included within the mass flow numerical model?

An important factor influencing equilibrium temperature of a given material is thermal diffusivity (m^2/sec), a measure combining the properties of heat capacity and thermal resistance to represent a given material's behavior with respect to thermal inertia. Materials with high thermal diffusivity have lower resistances but gain and release heat rapidly for a given density; materials with low thermal diffusivity have higher resistances but gain and release heat slowly. The impact on materials during heat gain is that for a given heat gain, materials with low thermal diffusivity do not as easily transfer and reject heat to their surfaces, resulting in increased stored heat and increased temperature. On the other hand, materials with high thermal diffusivities transfer and reject heat very rapidly to their surfaces, reducing stored heat and lowering temperature. The role of solar gain in the process is of interest because, looking singularly at the factor of thermal resistance, one might conclude that for an isolated cladding component subject to heat gain from insolation, decreasing thermal diffusivity while also increasing material thickness (to the benefit of decreasing conduction) would lower the resultant temperatures on its opposite side. However, given the property of diffusivity, we have to look at materials very differently and recognize that under these conditions a material with high diffusivity can actually be quite effective in releasing heat despite its thermal resistance. Aluminum, it turns out, is just such a material, with a thermal diffusivity among the highest of solid materials. Stone and brick, materials proposed in Ciampi (2003) as the most preferable for ventilated cladding, have thermal diffusivities that are extremely low among solids.

Moreover, a cladding material with a high thermal diffusivity and thinness in section releases heat more readily from each side when separated from the backup wall. In this case the combined impact of diffusivity and thinness suggests the sol-air equation (Eq. 3) is not a satisfactory prediction of resultant surface temperature for such thin materials with high diffusivity because it accounts for thermal behavior only on the exposed side; in a very thin material, heat transfer on the opposing side more immediately impacts the exposed side's temperature, a property that would increase with increasing thermal diffusivity.

3.0 COOL SKINS BEHAVIOR

Moving the focus from mass flow to equilibrium temperature, it may be hypothesized that the cladding layer's ability to maintain the lowest possible temperature with respect to insolation is perhaps the most important indicator of potential ventilated cladding cooling performance. Hypothetically, a lower cladding temperature would tend to transfer less heat to the drainage plane by radiation, and given the lower, more turbulent flow characteristics within the air cavity, the cladding temperature likely has an increased influence on air cavity temperatures and convective heat transfer. The numerical model needed to model cavity air flow while accounting more thoroughly for cladding temperature would be quite complex. For this reason the research presented here focused on CFD simulation in order to study and generalize the relationship between solar radiation, cladding equilibrium temperature, and drainage plane temperature.

In this series of experiments, a computational fluid dynamics model was developed using the dimensions, boundary conditions, and heat inputs represented in Figure 4. For these tests (as well as for subsequent tests) Autodesk Simulation CFD 2013 was used to conduct the thermal simulations, and the the simulations were run provisionally for 100 iterations, with further iterations pending to assure adequate convergence. The tests were set up to compare the thermal equilibrium of ventilated cladding systems versus a non-ventilated cladding system, and in each of the tests backup wall assemblies were modeled realistically with gypsum sheathing, an 3.5" air cavity presuming a framed wall, and a gypsum wall board finish on the interior. The ventilated cladding system had panels that were 44cm in height with gaps of 1.4cm between them. The depth of the ventilation cavity was 5cm. A system with open joints was tested based on the conclusions of past research that recognized the increased ventilation and heat rejection in open joint systems (Gibson 2013).

Air flow on the exterior of the model was allowed to freely convect during the simulation, and radiant heat transfer was included in the solution. The starting environmental temperature for the air volume was 85F. The interior wall used a fixed temperature boundary condition to simulate the effect of an interior temperature held at a constant rate via climate control. The temperature was elevated to represent the effects of an air film.

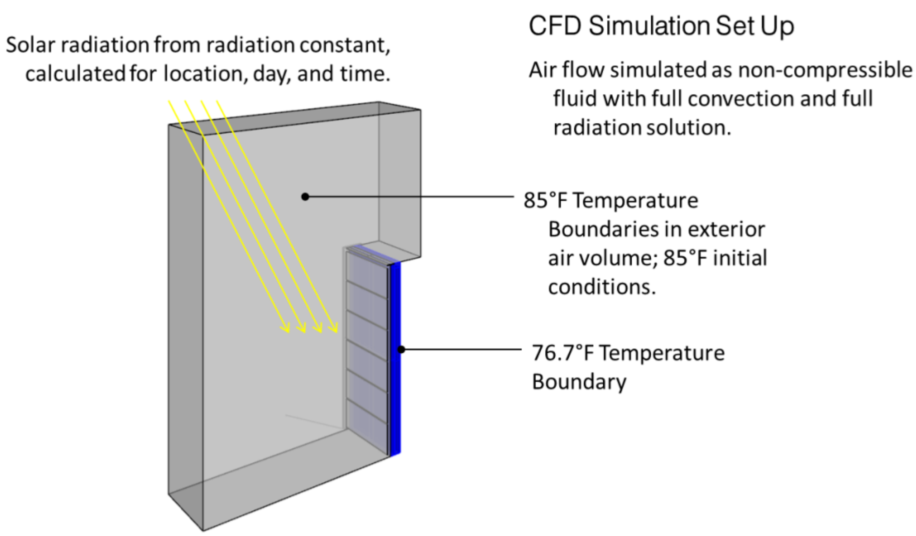

Figure 4: A diagram of the Computational Fluid Dynamics model is represented here, showing boundary conditions and critical materials.

3.1 Insulation Variations

As discussed earlier, insulation has the effect of thermally isolating the cladding during periods of heat gain. In a wall with unventilated cladding, the cladding conducts heat through the wall assembly to the interior. Insulation, while reducing this rate of conduction, also increased gained and subsequently stored heat in the cladding, raising the cladding temperature. In other words, introducing increasing amounts of insulation presents complex thermal behavior. On one hand, conduction is slowed. Yet on the other, for this increase in thermal resistance the cladding will reach higher temperature equilibriums, increasing conduction and reducing somewhat the benefits of increased thermal resistance. It is significant also that the sol-air equation does not recognize these two countering effects because the sol-air equation focuses on the material of the properties of the cladding and not the dynamic behavior of the entire assembly.

A series of CFD simulations was conducted comparing the equilibrium temperatures of ventilated and non-ventilated cladding systems under solar gain. Solar geometry for June 21 at 1:00p was used for radiation input. The ventilated and non-ventilated configurations were simulated without insulation, and with 25mm, 50mm, and 75mm depths of extruded polystyrene insulation. High-pressure laminate (HPL) cladding of 1cm thickness was used for the simulations, and a sheathed, uninsulated cavity wall was modeled behind the cladding as described previously. In lieu of exact physical properties for HPL, the material used in the simulation was a high density particle board of similar composition.

The results of the tests showed that indeed, increasing the insulation in the non-ventilated cladding models increased the equilibrium temperature of the cladding (Figure 6). When the heat transfer rate is calculated for these temperatures (using the conventional conduction equation and not CFD) the diminishing benefit of thermal resistance can be seen as a flattening in the reduction of heat transfer rate as insulation is thickened (Figure 7).

In the same tests, the ventilated HPL cladding remained at a relatively steady temperature as insulation was increased (Figure 6). While temperature increased at the drainage plane as insulation was increased, these changes were more moderate and did not result in a diminishing heat transfer reduction (Figure 7) as can be seen with the unventilated cladding. These tests also show that ventilating the cladding reduces teat transfer rates by 52% with 25mm insulation, 50% for 50mm insulation, and 50% for 75mm insulation (Figure 7). In other words, the reduction in heat transfer gained by ventilating the cladding is consistent regardless of the insulation depth.

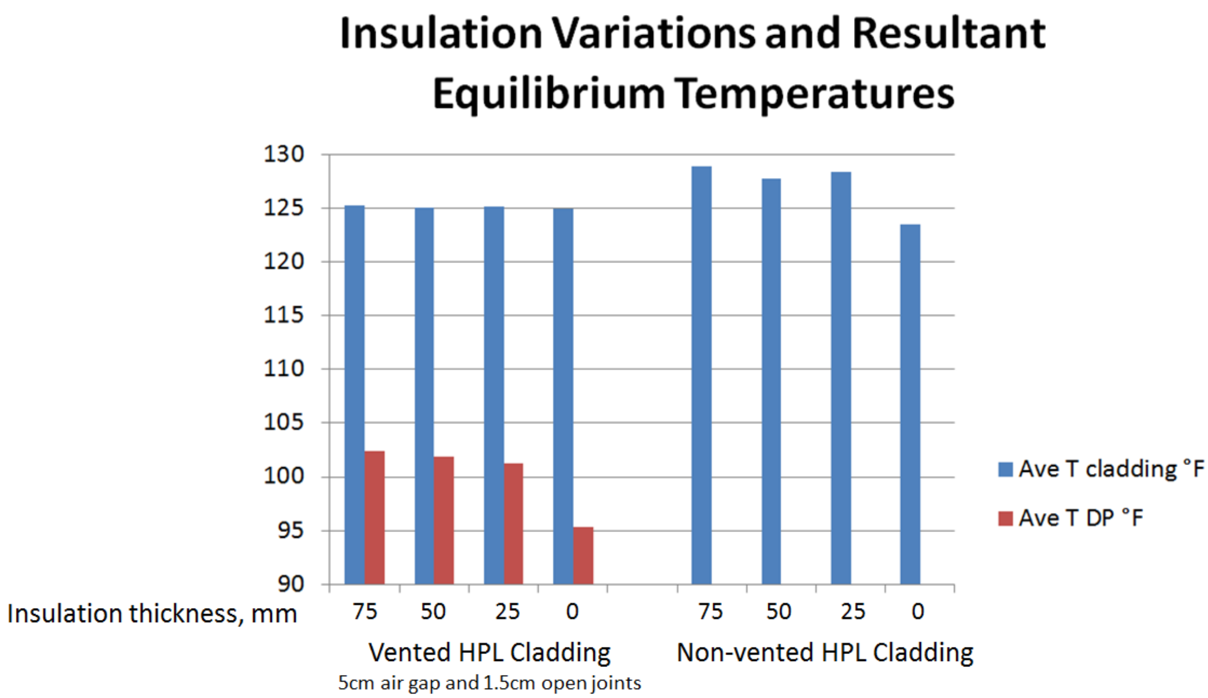

Figure 6: CFD simulations show that with non-ventilated cladding, increasing exterior insulation elevates the cladding temperature; ventilating the cladding (left) results in steady cladding and drainage plane temperatures, even while insulation depth is increased. Low temperatures on the exterior without exterior insulation (0mm) represent increased heat flow to the interior.

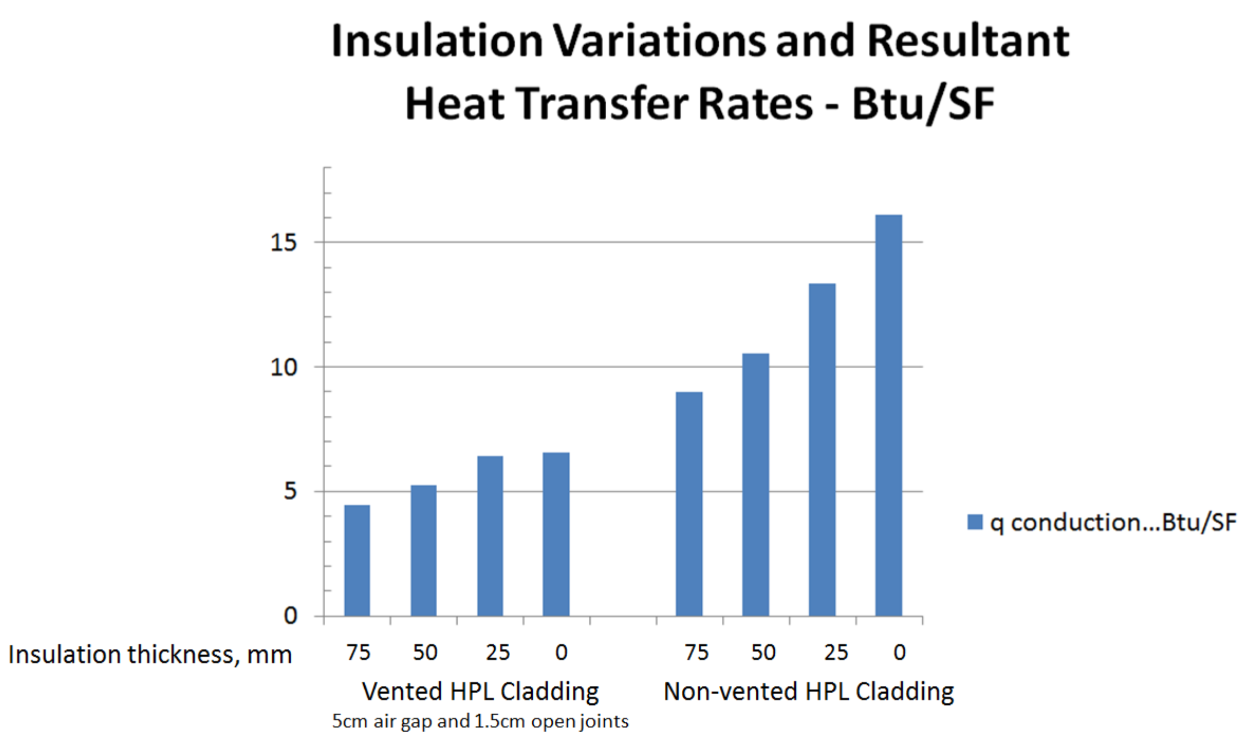

Figure 7: Ventilating the cladding reduces teat transfer rates by 52% with 25mm insulation, 50% for 50mm insulation, and 50% for 75mm insulation.

Evaluating insulation depths and their impact on cladding is of particular relevance today given changes to the International Energy Conservation Code (IECC) which now mandates continuous insulation for nearly all exterior wall assembly types, including in residential construction. In most cases this insulation will be expanded or extruded polystyrene insulation (commonly known as rigid insulation), as tested in these simulations. The results of these simulations suggest that ventilating the building cladding reduces heat gain through the wall assembly consistently, even as insulation is thickened. The simulations also suggest that, at least in terms of cooling season performance, ventilated cladding is preferable over non-ventilated cladding because of the diminishing performance benefits resulting from the isolation of heat gains in cladding.

3.2 Material Variations

Earlier in this paper it was discussed solar heat gain is typically factored into building energy flows (i.e. whole building energy simulation) using the sol-air equation (EQ. 3). In this manner, it is typical to emphasize a material's absorptivity in the solar spectrum as an important indicator of performance with respect to heat gain from the sun. The surface resistance of the cladding material is also a major factor in the sol-air equation.

On the other hand we may consider properties of cladding that relate to thermal storage and earlier we mentioned diffusivity and its relationship to equilibrium temperature. When considering the heat transfer properties of ventilated cladding, heat transfer is impacting both sides of the cladding and the cladding is relatively thin (at least compared to the total thickness of a wall assembly). The cladding's equilibrium temperature will be influenced not just by the elevation of its surface temperature from insolation, but also due to the rate at which heat enters, propagates through, and leaves the system. It may be presumed that materials diffusing heat more slowly would tend to retain more of this insolation, while materials diffusing heat more quickly will reject more heat. Absorptivity is still important in this process by influencing the initial response to solar radiation; however now we may consider diffusivity (mm^2/sec) as an important material property along with material thickness. Rather than apply diffusivity directly in calculation, we may discuss it alongside a set of CFD simulations. While CFD does not explicitly use diffusivity as a material property, diffusivity is manifested within CFD through the application of the heat equation to calculate heat propagation within material meshes using the components of conductivity, density, and heat capacity.

In order to compare equilibrium temperatures, three materials – aluminum, HPL (represented by hardboard), and granite – were modeled in CFD and each material variation was simulated in a ventilated and a non-ventilated configuration. Granite of middle-range color and absorptivity was used in lieu of limestone because an appropriate set of thermal parameters had not been identified for limestone at the time of testing. The model included 75mm of exterior insulation in the wall assembly. Solar geometry for June 21 at 1:00p was used for radiation input. In Table 1 the diffusivity of the materials simulated is shown, with high diffusivity values indicating more rapid propagation of heat within the material. Comparing values it can be seen that aluminum has a very high value compared with the other, and has a much higher diffusivity than stainless steel even though these are both metals. Limestone has the lowest diffusivity. Subsequently, these materials have different thicknesses when used in building cladding and Table 1 shows the thicknesses presumed for these tests. The parameter of thickness further compounds the effect of diffusivity because it increases the amount of heat gained stored within the material, which would predictably raise its equilibrium temperature if its diffusivity is very low. While aluminum is very thin (presumably good for equilibrium temperature) stone must be thicker when it is used in cladding because of its mechanical properties. This poses a liability. HPL is somewhere in between regarding thickness, though it has a high density.

TABLE 1: Diffusivity of Simulated Materials

	Thermal Diffusivity	Thickness Tested
Aluminum:	84.18 mm2/sec	2mm
Stainless Steel (304):	4.2 mm2/sec	-
Hardboard:	6.7 mm2/sec	10mm
Granite:	1.6 mm2/sec	30mm

It was observed in earlier tests that in ventilated cladding systems, cladding equilibrium temperature heavily influences the temperature of the drainage plane. Thus before referring to the drainage plane temperatures from the simulations, the temperatures on either side of the cladding may be discussed. The aluminum cladding resulted in the lowest cladding temperatures; in addition, the temperatures on both faces of the cladding were identical. Stone had the highest cavity-side cladding temperature, although this was within a degree of the exterior temperature. HPL showed very different results, reaching the highest exterior-side temperature of the three but with a difference of over 8°F across the cladding thickness. What may be gleaned from these results is that given the material properties of HPL and granite, the higher exterior temperatures indicate continued conduction of heat into the cavity at equilibrium temperature. Aluminum shows a very different pattern; in this case aluminum's temperatures suggest a scenario in which heat is propagated so thoroughly that it can be conducted in either direction. When we consider heat loss at the exterior cladding site by convection and emission, the ability of the aluminum to conduct heat from the cavity (even during a sunny day) presents an important advantage.

TABLE 2: Ventilated Cladding Temperatures, Exterior Side Vs. Cavity Side

	$T_{cladding}$ Ext, °F	$T_{cladding}$ Cavity, °F	T_{diff}, cladding, °F
2mm Alum - Vent	89.2	89.2	0.0
10mm HPL - Vent	115.9	107.7	8.2
30mm Granite - Vent	110.6	109.6	1.0

When drainage plane temperatures are assessed (Figure 8) the performance of the three materials is predicted by the resulting cavity-side cladding temperatures: aluminum has the lowest drainage plane temperature followed by HPL and granite. Comparing temperatures of the ventilated versus unventilated tests in Figure 8 and Table 3, it may be observed that granite benefits the most from ventilation (a 47% reduction in heat transfer) and aluminum, with a very low drainage plane temperature to begin with, has a smaller margin of improvement with ventilation (21% reduction). Comparing the worst performing simulation (stone, unventilated) with the ventilated aluminum shows a 64% reduction, realized by selecting a better performing material and ventilating the cladding.

Another interesting result from these simulations was the comparison of the resultant temperatures to the temperatures given by sol-air calculations (Figure 8). These calculations were made by extrapolating the solar insolation value from the CFD simulation and using it separately with material properties to calculate sol-air temperature (using EQ 3). In Figure 8 two sol-air figures are shown. One uses the 'general absorptivity' which equals the reference emissivity value of the material in CFD. Another value shown uses the correct solar absorptivity for the material, which is its absorptivity in the solar radiation spectrum. CFD does not account for changes in emissivity according to temperature when it calculates radiative heat transfer, and thus both values are calculated manually for comparison. It may be seen that because of the conductivity of aluminum and stone, the absorptivity doesn't change significantly between calculations using general and solar absorptivity. HPL is less conductive and thus the correction in absorptivity results in a greater difference in sol-air temperature. For this reason we may infer that the CFD equilibrium temperatures for HPL may be lower in reality than those shown. A more significant observation is that the sol-air temperatures are very different than the equilibrium temperatures resulting in CFD, and the materials perform in a different order. Aluminum and stone in the unventilated CFD simulation reach higher temperatures than sol-air, while HPL is lower. While HPL and stone perform at a lower temperature than sol-air in the ventilated CFD simulation, aluminum's equilibrium temperature remains higher in the CFD simulation than sol-air temperature.

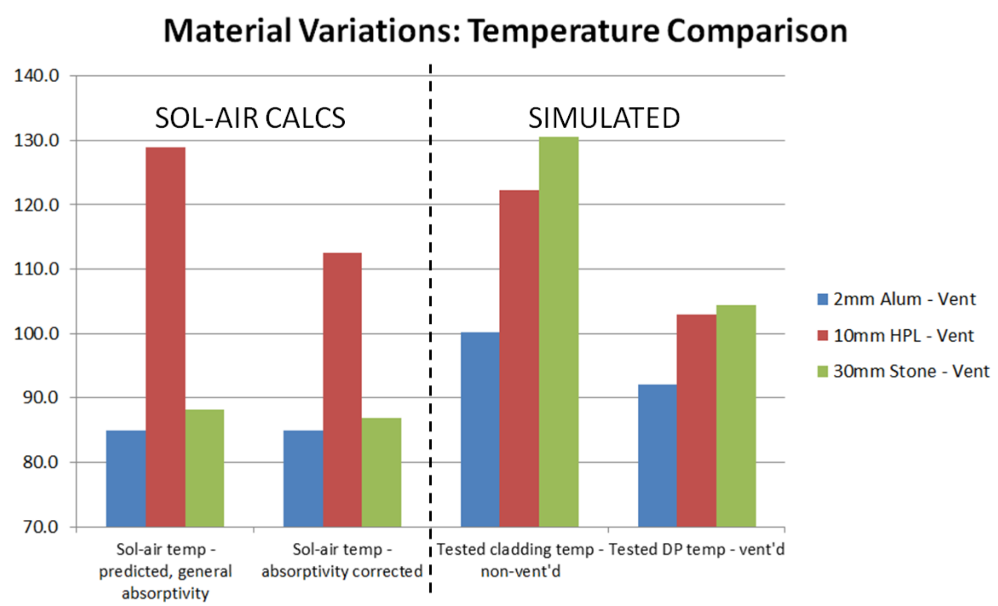

Figure 8: Comparison of the resultant temperatures from CFD simulation to the temperatures given by sol-air calculations.

TABLE 3: Heat transfer rates from material simulations

	q unvent'd cladding, Btu/h*ft^2	q vent'd cladding*, Btu/h*ft^2
2mm Alum - Vent	1.38	1.09
10mm HPL - Vent	2.58	1.52
30mm Granite - Vent	3.04	1.60

*ventilated cladding q was calculated from drainage plane to interior

It may be summarized that sol-air calculations do not align very well with the equilibrium temperatures observed in the simulations, confirming the heat transfer dynamics at play beyond the sol-air calculation are significant. The property of thermal diffusivity in conclusion is an important indicator of a material's ability to reject heat when it is used in ventilated cladding.

3.3 Incident Solar Variations

Two dates were selected to examine differences in solar geometry and insolation values relative to cooling season performance: June 21st, the summer solstice, and September 21st, the fall equinox. The models were oriented to the south and thermally isolated objects in the model prevented exposure of the sides of the models to additional radiation during the simulations. Additionally, the models were tested with solar geometry and insolation values for noon, 1:00p, 2:00p, and 3:00p local time (as controlled in the simulation software). It should be noted that insolation values used in the CFD simulation are based on the solar constant and do not account for atmospheric, climate, or weather-related effects.

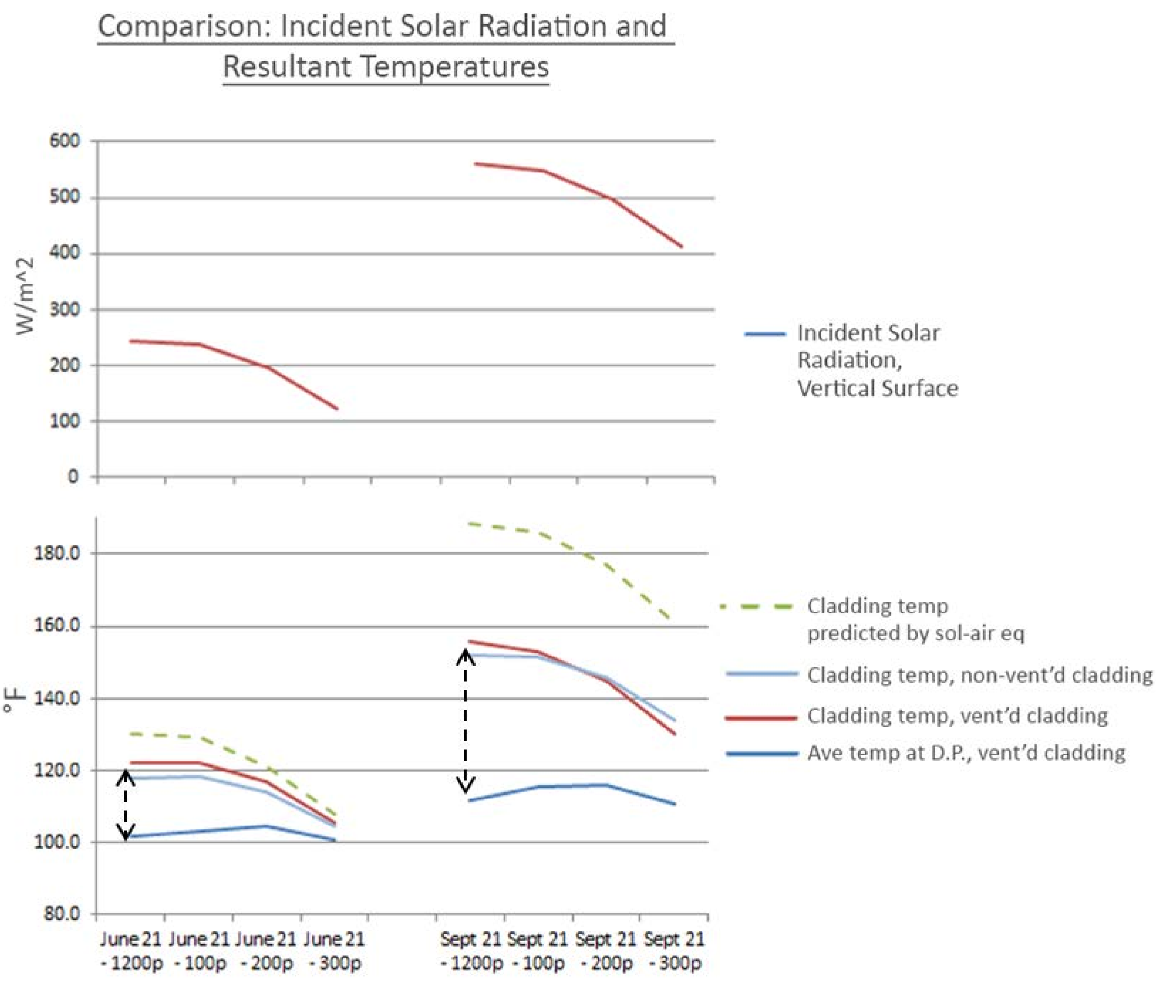

Figure 9: Graph comparing vertical surface incident radiation and equilibrium temperatures from CFD analysis from eight different day/time geometries. Note the insolation curves correlate closely to simulated cladding temperatures. The vertical arrows highlight the reduction in temperature at the drainage plane as it compares to different day/time simulations. This reduction correlates closely to the vertical incident solar radiation.

Results of the insolation variations showed clear correlations between vertical insolation quantities and the cladding temperature of the ventilated and non-ventilated cladding systems (Fig. 9). Insolation values used as heat inputs in the CFD program were used to separately calculate the sol-air temperature according to the common sol-air equation (Eq. 3) and these are also shown on the graph in Fig. 9, although it should be noted that these values are higher than the equilibrium temperatures calculated by CFD, presumably because the sol-air equation does not account for any heat losses due to convection and radiation. Temperatures at the drainage plane for the ventilated cladding model were much lower than non-ventilated cladding temperatures, and this reduction in drainage plane temperature increased as the magnitude of insolation increased. Notably, this relationship between temperature reduction and with increased insolation magnitude was predicted by the numerical model developed in Ciampi (2003). The correlation of incident solar radiation values to the reduction in heat transfer ‘q’ was 0.99 in June and 0.97 in Sept for the simulation data.

A particular question arose from the drainage plane temperatures during different times of the day – the resultant temperatures were quite flat in comparison to the cladding temperatures. This flatness perhaps indicates the drainage plane temperature is influenced independently by the exterior ambient temperature. However, the difference in drainage plain temperature for the ventilated cladding versus the non-ventilated cladding correlates very closely to the quantity of insolation impacting the cladding (Table 4). In other words, the reduction in temperature at the drainage plane when the cavity is ventilated, presumably as a result of heat losses due to convection and radiation at the cladding, is linked to insolation. We may then predict that over the course of the year, as insolation increases and decreases for the cladding, the heat transfer mechanisms driving temperature reduction at the drainage plane will increase and decrease correspondingly. Moreover, the impact of ventilated cladding is suggested to be consistent and predictable throughout annual changes in insolation.

4.0 EVALUATING PERFORMANCE IMPACT

In the previous section it was argued that the performance benefits of a ventilated building skin will persist throughout the cooling season, during times of the day where solar radiation is significant. The question arises, how can these observations from the instantaneous CFD simulations be introduced into an annual energy simulation to assess the impact of a ventilated building skin over the course of a season? What about a year?

It was discussed earlier that from the CFD simulation, the amount of heat transfer reduced by the ventilated skin correlates almost exactly with the amount of vertical surface incident solar radiation. Annual energy simulation tools separately calculate the gains on opaque surfaces from incident solar radiation, although this is referred to by various names among the different software platforms. It has been noted on a few occasions in this paper that the sol-air equation does not adequately represent the gains impacting thin materials; yet the sol-air method, which uses an excess temperature to account for radiation as a part of conducted heat gain, is the most feasible option with today’s computing power to evaluate the performance of a ventilated building skin over the course of the year. One may use a transient analysis using CFD, but given the complexity of the heat transfer mechanisms at work we may take an approach where we evaluate an assembly in CFD first to generalize its performance, and translate these results into an annual energy simulation.

For this study, Autodesk Ecotect has been used and these gains are simply referred to as ‘sol-air gains’ and abbreviated as ‘sQss.’ These hourly values are part of the hourly heat balance calculated in thermal simulation, and surface orientation, surface thermal resistance, and absorptivity are part of the equation used in the simulation engine (EQ. 4).

$sQss = R_{SO}\ (\alpha \cdot G)$ (EQ. 4)

Whereby R_{SO} = resistance of outside (cladding) surface, ℓ /k
α = absorptivity of outside (cladding) surface
G = incident solar radiation

The above equation is similar to EQ. 3 except it represents only the sol-air excess temperature, and it is subsequently added to the hourly exterior drybulb temperature by the simulation engine.

Having defined the opaque surface incident solar gains, we can use simulation results to assign a unit of sol-air heat rejected for every unit of insolation (q_{sr}/G), given the correlation of these two values. These values are shown in Table 4 along with the values for sol-air heat rejection and insolation (G). At this juncture there are two possibilities for applying this factor, which may be called the ‘sol-air reduction factor.’ We may construct a function to describe with some precision how this factor shifts with solar geometry and integrate this into the energy model. Or we may average these values into a single ‘sol-air reduction factor’ to produce a single, conservative figure to represent the reduction of heat gain by the ventilated building skin.

For the purposes of this discussion, we will continue with the average value, understanding that this is a conservative figure that will not represent the maximum amount of heat gain reduced. Another item of note is that the range of incidence (altitude and azimuth) varies greatly for exposed surfaces of buildings although the simulations presented here are limited to south-facing orientations. We are moving forward with the presumption that insolation (G) as it has been calculated is radiation incident on the vertical surface, and is translatable to other orientations. In other words, the presumption is made that east- and west-facing walls will have similar performance. Additionally, it is also convenient that in annual simulations, surface insolation (G) is based on weather data and thus the sol-air calculations used here also reflects daily weather conditions.

Table 4:

	Cool skins Sol-air reduced q_{sr}	**G**	**Sol-air reduction component SRC= q_{sr}/G**	**Sol-air reduction component SRC = q_{sr}/G AVE**
June 21 - 1200p	1.125	77.30	0.015	0.011
June 21 - 100p	1.037	75.48	0.014	
June 21 - 200p	0.655	62.03	0.011	
June 21 - 300p	0.235	38.75	0.006	
Sept 21 - 1200p	2.473	177.96	0.014	0.011
Sept 21 - 100p	2.124	173.92	0.012	
Sept 21 - 200p	1.638	157.95	0.010	

Sept 21 - 300p	1.108	130.92	0.008	

In order to integrate the sol-air reduction factor with the hourly sol-air data, an equation can be implemented (EQ. 5) that will calculate a reduced sol-air excess value.

$sQss_{reduced} = sQss - (SRC)(G)$ EQ. 6

Whereby sQss = solair excess temperature
G = incident solar radiation
SRC = solair reduction component or q_{sr}/G

From EQ. 6 we may introduce known values for the sol-air reduction component shown in Table 4 and develop the following expression, knowing that we can substitute for insolation (G) as it is solved hourly in the simulation:

$(SRC)(G) = (SRC)*(sQss/(R_{SO}*\alpha))= (SRC)/(R_{SO}*\alpha)*sQss$ EQ. 7

At this point we may note that SRC, R_{SO}, and α for a given application will be known values that may be introduced to this expression. In the next step we may combine EQ. 6 and EQ. 7.

At this stage, we may return to the example building shown in Figure 2. This is a generic commercial building located in Houston, Texas. It has approximately 19,200 square feet of floor area (4,800 square feet per floor) and its envelope follows the prescriptive envelope requirements of the IECC, including a window area of 30% (in between the prescriptive 20 to 40% range). It is presumed this building is zoned by floor. Consider the second floor zone of this building for discussion. We can extract from an annual energy simulation that the total cooling loads for this zone, not including internal loads, will be 33.5 MBtu of cooling. During the cooling season (March to October in this climate), the loads from sol-air i.e. those contributed by direct gains on the opaque building envelope, are 2.2 MBtu. Looking at loads annually, it is easy to dismiss the direct gains as insignificant, however these loads play an important role for this zone during the swing seasons and during peak cooling hours. This is also a very warm climate whose temperatures exceed the comfort zone on a typical basis, even during the night; so this application is intended to show a realistic impact. Presuming this example has a non-ventilated HPL cladding system, we will use the example at this point to explore the impact of a ventilated HPL building skin. CFD simulation was used to study equilibrium temperature for this assembly in a ventilated versus non-ventilated configuration and was shown in Table 4.

Returning to EQ 6. and EQ. 7, we may combine these expressions into the following expression:

$sQss_{reduced} = sQss - (SRC)(G) = sQss – ((SRC)/(R_{SO}*\alpha)*sQss)$ EQ. 8

Whereby R_{SO} = resistance of outside (cladding) surface = 0.05284 Btu/°F*h*ft^2
α = absorptivity of outside (cladding) surface = 0.4
SRC = solair reduction component or q_{sr}/G = 0.011
Note: SRC is calculated from simulated values elaborated in Table 4.

Yielding:

$sQss_{reduced} = sQss – (0.52)(sQss) = (0.48)(sQss)$ EQ. 9

This provides a reduction factor that may be applied to the hourly sol-air excess gains for all vertical surfaces, regardless of their orientation – a point discussed in detail earlier in the paper. Applying the factor that we just calculated in EQ 9 we may see the total direct gains through the opaque envelope reduced from 2.2 MBtu in the cooling season to 0.9 MBtu.

Further, we can observe the monthly reduction in cooling loads over the course of the year, shown in Figure 10. The monthly reduction in gains as a result of the ventilated skin is modest over the course of the hot summer months, but represents a sizeable portion of gains in the swing seasons (spring and fall) when the building is the closest to passive operation. In July the reduction from the ventilated skin is only 2% of loads, but in May this number increases to 4%, and by March this figure reaches 44%, and October this reduction is 10%. A common question of the ventilated skin strategy relates to winter time performance – shouldn't there be some significant heat loss from ventilating the skin in the winter? In reality, even in Houston in this example, the heating loads reach a magnitude that the loss of heat gain in the skin (by a reduction in skin temperature) is quite minor: only about 0.7% of the losses. These figures may shift in some climates but this demonstrates the importance of this strategy in temperate areas, even when winters are cold (albeit short).

Secondly, the solair gains contribute to 21% of the peak cooling load in the simulation. Reducing these gains by ventilating the building skin would reduce the peak load in this zone by 10%, which is a substantial contribution to HVAC sizing and perhaps to comfort.

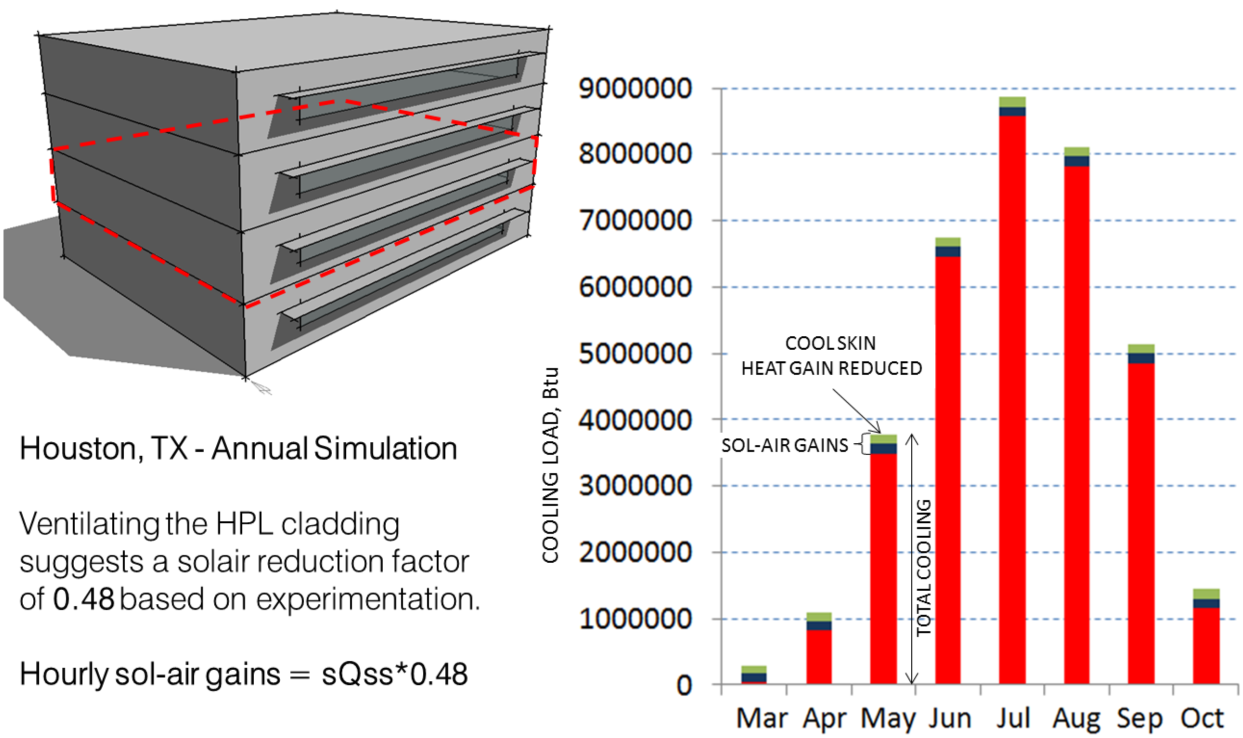

Figure 10: Example building located in Houston Texas, showing a simulation of the second floor zone and the total cooling load, sol-air gains, and the amount of gains reduced by a proposed ventilated skin (in green). Note that considering passive operation, this reduction in solar gains is particularly useful in the swing seasons when cooling loads are modest. Not shown in the graph is that sol-air gains contributed 21% to the maximum cooling load; given this calculation, the maximum cooling load for this zone would be reduced 10% as a result of the ventilated skin.

In conclusion to this evaluation, we can see that the most important result of using the ventilated skin is a reduction in peak cooling load (10%) and significant reductions in monthly swing season cooling loads (44% in March and 10% in October) which may assist the building in passive operation. Ventilating a building skin may not have very large immediate economic impacts, but it may be a cost-neutral modification to the overall building envelope and can have an impact similar to the addition of blinds or shading devices.

5.0 CONCLUSIONS

In conclusion, the evidence presented in this study supports the following points:

- There is significant evidence that for most conceivable materials and applications, ventilated building skins with open joints will result in some degree of reduced heat transmission through the vertical wall assembly during periods of solar heat gain. Understanding the equilibrium temperature of an assembly for a given solar load is a good predictor of performance, not only the dimensions of the cavity.
- Materials that have a low absorptivity are preferable for ventilated cladding systems. We may also conclude that materials with high diffusivity and overall low mass will reduce the tendency of the cladding system to store heat during periods of heat gain, leading to increased equilibrium temperature. It may also be noted that heavier cladding systems have increased backup structures that, by introducing more thermal bridges and more mass into the cavity, will increase the retention and transfer of heat.
- When using continuous rigid insulation it is important to ventilate the cladding to maximize the performance of the insulation in reducing heat transmission during the cooling season.
- The sol-air method of introducing insolation gains to the conduction of heat through wall assemblies has shortcomings when evaluating very thin materials. It may also not be used alone for the evaluation of ventilated skins.
- The best approach to holistically evaluate the performance of a ventilated cladding assembly is to generalize its performance using CFD simulation, and use results to define a reduction factor for sol-air gains. This reduction factor can then be integrated into an annual energy simulation.
- Ventilated building skins are a promising energy reduction strategy for multi-level, multi-zone, skin-load dominated buildings in warm climates with substantial insolation loads. Yet because of the cost of electricity ventilated building skins must be sought to solve several performance problems at once, including durability of cladding materials and continuity and performance of the weather barriers. This latter topic is beyond the scope of this paper but if a ventilated skin is pursued for other reasons, there is substantial evidence that cooling season performance benefits can be realized and quantified.

Overall, the author would like to note that this is an ongoing study and the intent is to continue the tests with more precise CFD modeling and with increased scope, focusing on aluminum and metal systems. CFD iterations were limited to 100 iterations for processing time, and these tests should be increased to gain increased certainly regarding the CFD results. It may also be noted that other researchers in yet-to-be-published works have come to different conclusions regarding the best materials for ventilated building skins and it will be interesting to compare these results and how they are related to differences in material, testing, and climate. Lastly, the author intends to continue testing using prototypes and live tests to confirm conclusions made by CFD and calculation wherever possible.

REFERENCES

Ciampi, M., Leccese, F., Tuoni, G. (2003). “Ventilated facades’ energy performance in summer cooling of buildings.” *Solar Energy,* 75, 491–502.

Ciampi, M., F. Leccese, G. Tuoni. (2005). “Energy analysis of ventilated and microventilated roofs”
Solar Energy 79 (2005) 183–192

Gibson, Michael. (2013) “Cool Skins: Exploring the Cooling Potential of Light-Weight, Layered Wall Systems.” *Visibility of Research: Proceedings of the 2013 ARCC Conference, Charlotte NC, March 2013.*

Giancolaa, E., C. Sanjuana, E. Blancob, M.R. Herasa. (2012) “Experimental assessment and modelling of the performance of an open joint ventilated facade during actual operating conditions in Mediterranean climate” Energy and Buildings 54, 363–375

Marinosci, C., P.A. Strachan, G. Semptrini, and G.L.Morina. (2011) “Empirical Validation and Modeling of a Naturally Ventilated Rainscreen Façade Building.” *Energy and Buildings,* 43, 853-863.

Suárez, C., P. Joubert, J.L. Molina, F.J. Sánchez. (2011). “Heat transfer and mass flow correlations for ventilated facades.” *Energy and Buildings,* 43, 3696–3703.